Cellulose (2020) 27:611–620
https://doi.org/10.1007/s10570-019-02833-y

ORIGINAL RESEARCH

# Hygroscopic swelling of moso bamboo cells

**Qi Chen · Changhua Fang · Ge Wang · Xinxin Ma · Meiling Chen · Shuqin Zhang · Chunping Dai · Benhua Fei**

Received: 3 August 2019 / Accepted: 30 October 2019 / Published online: 5 November 2019
© Springer Nature B.V. 2019

**Abstract** Bamboo is a natural cellulosic material which is strongly reactive to water. Its hygroscopic behavior affects almost all other physical and mechanical properties of bamboo. This study investigated the hygroscopic swelling of moso bamboo (*Phyllostachys edulis*) cells in response to changes in environmental humidity using a confocal laser scanning microscope. The swelling strains of fiber, vessel and parenchyma cells were obtained and compared. The interactions between adjacent cells were also analyzed. The results demonstrated that the swelling strain of the cell walls increased with relative humidity, and was independent of its location and orientation, but dependent on the cell type. The absolute swelling of fiber cells was highest among all cells because of dominantly high fiber wall thickness. In contrast, the relative swelling of fiber cells was lowest due to constraint of adjacent fibers. Fiber cells governed the deformation and movement of other cell lumens. The difference between tangential and radial swelling of bamboo was insignificant compared to that of wood, possibly due to the similar microfibril angle in both directions, the circular cell shape and the random embedment of vascular bundles.

**Keywords** Bamboo · Hygroscopic swelling · Cell wall · Cell lumen · Moisture adsorption · Dimensional stability

Q. Chen · C. Fang · G. Wang · X. Ma ·
M. Chen · S. Zhang · B. Fei (✉)
Department of Biomaterials, International Centre for Bamboo and Rattan, No. 8, Futong East Street, Chaoyang District, Beijing, People's Republic of China
e-mail: feibenhua@icbr.ac.cn

Q. Chen · C. Fang · G. Wang · X. Ma ·
M. Chen · S. Zhang · B. Fei
SFA and Beijing Co-Built Key Laboratory of Bamboo and Rattan Science and Technology, State Forestry Administration, Beijing, People's Republic of China

Q. Chen · M. Chen · C. Dai (✉)
Department of Wood Science, Faculty of Forestry, University of British Columbia, Vancouver V6T1Z4, Canada
e-mail: chunping.dai@ubc.ca

## Introduction

Bamboo is a natural composite material that has been widely used in construction materials, daily used commodities, membrane supports, biopolymer films, and many other applications (Chen et al. 2019; Fang et al. 2018; Wegst 2008; Ribeiro et al. 2016; Khalil et al. 2018; Du et al. 2018; Le Phuong et al. 2019). As a hygroscopic material, bamboo undergoes dimensional changes in response to varying environmental humidity, i.e., it swells in a high relative humidity (RH) and shrinks in a low RH (Lv et al. 2019). Over the past few years, researchers have performed macro-scale studies on the transverse dimensional changes of bamboo of different heights and species (Ahmad and Kamke 2005; Anokye et al. 2014; Erakhrumen and Ogunsanwo 2009; Wahab et al. 2012a, b). These studies have revealed some information on the expansion of bamboo at the macro scale; however, the mechanism involved in the swelling of bamboo cells, which is probably the main reason for bamboo swelling, is not clearly defined. Bamboo is mainly composed of three types of cells: fiber, vessel, and parenchyma cells. Fiber cells have solid multi- and thick- walled structures with tiny lumens, while parenchyma cells have fragile multi- and thin- walled structures with large lumens (Chen et al. 2018; Habibi et al. 2015). Of these three types of cells, vessel cells have the thinnest walls and the largest lumens (Yang et al. 2011). Since these cells, with evidently different morphologies, are responsible for the swelling of bamboo, it is, therefore, necessary to obtain a fundamental understanding of their swelling behaviors.

Fiber, vessel, and parenchyma cells in bamboo exist adjacent to each other. The cells adjacent to fibers are parenchyma cells and vessel cell, or parenchyma cells and sieve cells. The cells adjacent to vessel cell are fiber and parenchyma cells. The cells adjacent to parenchyma cells can be either fiber or vessel cells, or sometimes other parenchyma cells (Jiang 2007). Previous studies have revealed that the dimensional change of cells in wood was strongly affected by the adjacent cells (Sakagami et al. 2007; Taguchi et al. 2010). Sakagami et al. (2007) found that when the moisture content decreased by 0.77%, one cell wall decreased by 0.32 μm, while its adjacent cell wall increased by 0.16 μm. Taguchi et al. (2010, 2011) also reported that cell wall deformation varied from cell to cell, and that some cells even shrank during water adsorption. Since the interaction between adjacent cells is significant, it is essential to consider the interaction of different bamboo cell types.

The dimensional changes of cells are reflected at the macro scale. For example, in wood, the swelling of cells is higher in the tangential (T) than in the radial (R) direction (Taguchi et al. 2010, 2011), and thus wood has a larger T-dimensional change at the macro scale (Patera et al. 2013; Rafsanjani et al. 2012, 2013, 2014; Taguchi et al. 2010; Yamashita et al. 2009). However, in bamboo, the direction of larger shrinkage at the macro scale is still unknown. Wahab et al. (2012a, b) demonstrated that shrinkage in the T direction was larger than in the R direction, while Erakhrumen and Ogunsanwo (2009) reported the reverse result. Furthermore, studies by Ahmad et al. (Ahmad and Kamke 2005; Anokye et al. 2014) have illustrated the variability in the direction of larger shrinkage. There are reasons to believe that these uncertain transverse changes of bamboo are related to the changes of bamboo cells. Thus, interpreting the deformations at the cellular level could perhaps contribute to the understanding of the transverse changes of bamboo at the macro scale.

In this study, the swelling behaviors of bamboo cells were investigated with the following objectives: (1) to determine the swelling of different types of bamboo cells and the variation among them; (2) to define the interaction between the adjacent cells; (3) to explain the macro swelling behavior of bamboo from the cellular level.

## Materials and methods

### Specimen preparation

Moso bamboo (*Phyllostachys edulis*) with an age of 5 years was obtained from Zhejiang Province, China. Bamboo strip of 2 × 2 × 10 mm (tangential × radial × longitudinal) was cut from the internodes of the bamboo culm located at a height between 1.5 m and 2.5 m. The transverse surface of the sample was cut using a microtome, and the thickness of the slices was 10 μm. The slices were then placed on glass slides to obtain the representative elements, which should each consist of a complete vascular bundle and its surrounding parenchyma cells (as shown in Fig. 1). The representative elements were cut by hand under an optical microscope. Three representative elements were prepared.

### Microscopic observations

Before microscopic observation, the specimens were adjusted sequentially in different RH conditions and immersed in distilled water (Table 1). They were kept under each condition for three days. After the specimens reached equilibrium moisture content (EMC), they were taken out from the desiccators, placed on a microscope slide, and covered with a glass. Nail polish was then used to quickly seal the edges, and the entire slides were replaced into desiccators to dry the nail

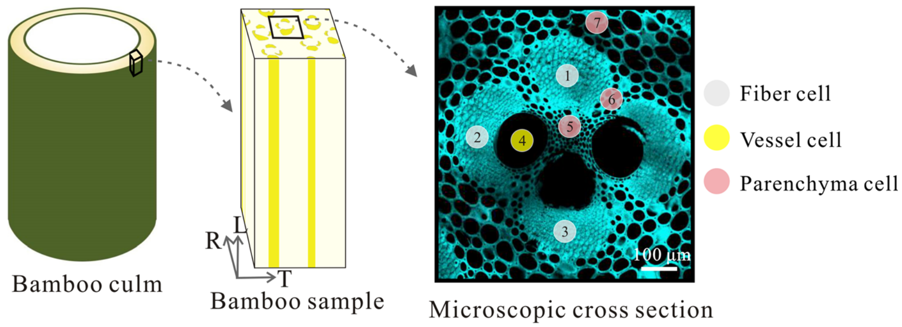


**Fig. 1** Sample and experimental configuration: schematic representation of observed sample prepared from cross-section of bamboo culm (grey refers to fiber cells, whereas yellow and red refer to vessel and parenchyma cells, respectively)

**Table 1** Relative humidity (RH) levels and the corresponding equilibrium moisture content (EMC) values of the experiments

| Solution | RH (%) | EMC[a] (%) |
|---|---|---|
| LiCl | 11 | 1.61 |
| $MgCl_2$ | 33 | 3.40 |
| NaBr | 57 | 6.49 |
| KCl | 84 | 13.60 |
| water | – | – |

[a]EMC values were obtained by a dynamic vapor sorption apparatus

polish. The transverse surfaces of cells were then observed by a confocal laser scanning microscope (CLSM, LSM 510 Mete, Zeiss). The images were captured using an oil immersion lens (100 ×) for fiber cells, and an oil immersion lens (63 ×) for vessel and parenchyma cells. To understand the interaction between adjacent cells, each type of cell was divided into several regions (regions of interest, ROIs) based on the relative structural configurations of different cells. The details of these ROIs are presented in Fig. 1 and Table 2. The test conditions were constant at room temperature. Once the testing was completed, the glass cover was removed, and the specimens were placed into the next RH conditions to achieve equilibrium.

## Image analysis

Images from the CLSM were measured and analyzed using ZEN 2.6 software (blue edition) provided by the instrument producer. The schematic figure of the measurement of the fiber cell is shown in Fig. 2a. Since it was difficult to distinguish the cell edges, the cell lumens were chosen as the feature points. A straight line was drawn to join the cell lumens of the adjacent cells, and the intensity of each dot on this line was obtained. The wave crest of this line corresponded to the cell wall, while the wave trough was related to the cell lumen, and the width of the wave crest was the thickness of the cell wall. Fiber cell lumens are too small to measure, and thus only the cell wall thickness was measured. The schematic figure of the measurement of the parenchyma cell is shown in Fig. 2b. Every parenchyma cell has cell corners which were regarded as the feature points. A straight line was drawn to join the cell corners on a diagonal. The width of the wave crest was the thickness of the cell wall, while the width of the wave trough was the diameter of

**Table 2** The cell type, adjacent cells and number of measurements (cell wall and cell lumen) in different regions of interest (ROIs)

| Cell type | ROIs | Adjacent cells of this region | Number of measurements | |
|---|---|---|---|---|
| | | | Cell wall | Cell lumen |
| Fiber cell | 1 | Parenchyma cells | 39 | – |
| | 2 | Parenchyma cells, vessel cell | 31 | – |
| | 3 | Parenchyma cells, sieve cells | 46 | – |
| Vessel cell | 4 | Parenchyma cells, fiber cells | 39 | 36 |
| Parenchyma cell | 5 | Vessel cells, fiber cells | 65 | 78 |
| | 6 | Fiber cells | 28 | 27 |
| | 7 | Parenchyma cells, fiber cells | 114 | 65 |

**Fig. 2** Illustrations of distance measurement for **a** fiber cell and **b** parenchyma cell

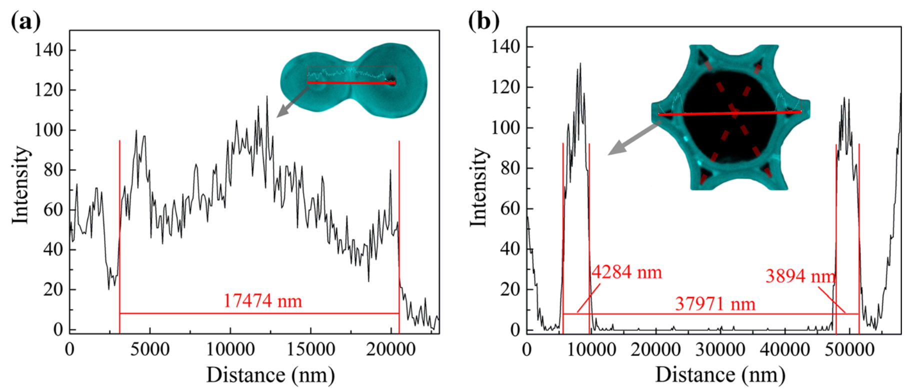


the cell lumen. The measurements of vessel cells were comparable to those of the parenchyma cells. The measured numbers of different ROIs are exhibited in Table 2. The swelling change for different cells was calculated as follows:

$$S = \frac{D_{RH} - D_{11}}{D_{11}} \quad (1)$$

$$S_A = \frac{D_{RH} - D_{11}}{MC_{RH} - MC_{11}} \quad (2)$$

$$S_R = \frac{S}{MC_{RH} - MC_{11}} \quad (3)$$

where $S$ (%) is swelling strain. $D_{RH}$ and $D_{11}$ represent the diameter values of cell wall or lumen at RH% and 11%, respectively. $S_A$ (nm/%) is absolute swelling per percentage of moisture content (MC). $MC_{RH}$ and $MC_{11}$ are the moisture contents of bamboo at RH% and 11%, respectively. $S_R$ (%/%) is relative swelling per percentage of MC (Rafsanjani et al. 2014).

## Results

### Swelling strains of fiber cells

The strains of the fiber cell wall at different ROIs as a function of RH are shown in Fig. 3. In general, during water adsorption, the cell wall expanded and reached the maximum after immersion in water. However, a small number of cells shrank at low RH. These cells might be squeezed by their adjacent cells (Sakagami et al. 2007). The strain varied significantly from cell to cell as evidenced by large error bar variation. Since the main variation among ROIs 1, 2, and 3 was adjacent

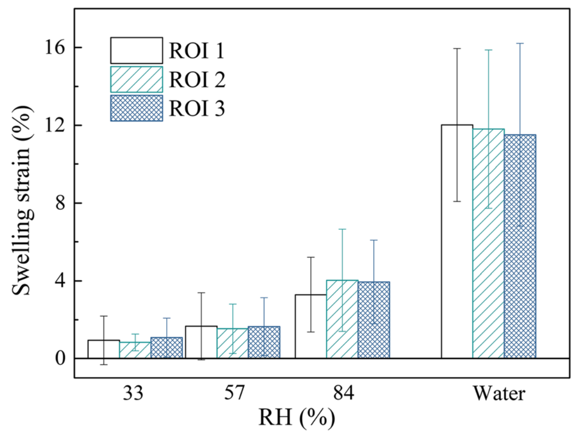


**Fig. 3** Swelling strains of fiber cell wall in ROIs 1, 2, and 3 at different RH conditions

cells, differences in these strains were insignificant, which implies that the fiber cells were not affected by the types of adjacent cells.

### Swelling strains of vessel cell

Figure 4a shows the swelling strains of the vessel cell wall close to the parenchyma cell side, as it was difficult to distinguish the cell edge at another side (close to the fiber cell). The cell wall of vessel cell increased linearly with the increase of RH.

To investigate the effect of adjacent cells on the swelling of vessel cell lumen, a line was drawn across the middle of fiber bundle and the middle of parenchyma cell area, and the orientation was set as 0°, with orientation 90° being perpendicular to this line (Fig. 4b). The swelling strains of the cell lumen at different orientations are shown in Fig. 4b. The strain decreased as the orientation changed from 0° to 90°, and had negative

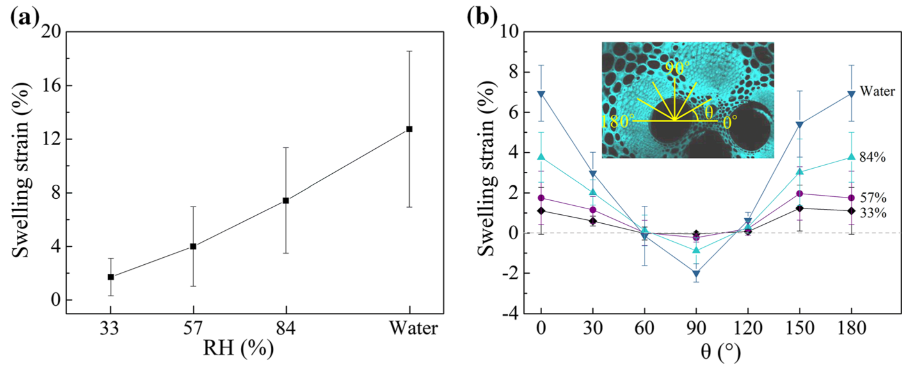


**Fig. 4** **a** Swelling strains of vessel cell wall at different RH conditions, **b** relationship between swelling strains of vessel cell lumen and adjacent cells at different RH conditions. The adjacent cells were fiber cells at 90° orientation, while they were parenchyma cells at 0° (180°) orientation

values at 90°. In contrast, the strain increased as the orientation shifted from 90° to 180°. For example, at 84% RH, the mean strain decreased over the 0–90° bracket, ranging from 3.76% to − 0.88%, and then increased back to 3.76% over the 90°–180° bracket. Therefore, the maximum increment of cell lumen was at 0°, and the greatest decrement was at 90°.

### Swelling strains of parenchyma cells

The results of vessel cell suggested that the swelling of the cell lumen was affected by the fibers. Therefore, the orientation of parenchyma cells was redefined based on the fiber effect. The orientations were categorized as follows: either parallel or perpendicular to the fibers (Fig. 5a). In this case, the orientations were not defined by absolute values such as 0° or 90°, but rather by ranges. It was in the parallel orientation if the straight line that joined the diagonal cell corners landed in a parallel area (blank area in Fig. 5a); otherwise, it was in the perpendicular orientation (shaded area in Fig. 5a). The parallel areas and perpendicular areas of ROIs 5–7 are shown in Fig. 5a, and the swelling strains of cell wall and cell lumen in these regions are shown in Fig. 5(b–d).

*ROI 5* The swelling strains of parenchyma cells in ROI 5 are shown in Fig. 5b. The strain of cell wall increased with the RH, and the two orientations had similar strain values. Like the fiber cells, some parenchyma cells also shrank during adsorption. The cell lumen was influenced by fibers that were located above it, and the lumen swelled when it was parallel to fibers and shrank when it was perpendicular to fibers. The expansion in parallel direction was approximately equal to the shrinkage in perpendicular direction. The area of cell lumen therefore stayed presumably constant.

*ROI 6* The swelling strains of parenchyma cells in ROI 6 are shown in Fig. 5c. The strain of the cell wall increased, and there was no difference in the strain of the two orientations. This was similar to the cells in ROI 5, but the increment was higher than that of ROI 5. The cell lumen increased slightly in the parallel direction but decreased significantly in the perpendicular direction, and the shrinkage was higher than that in ROI 5 or 7. Specifically, at 84% RH, the mean shrinkage strain in ROI 6 was 4.14%, which was higher than the strains in ROI 5 (1.56%) and ROI 7 (0.65%). Since the increment in the parallel direction was less than the decrement in the perpendicular direction, the area of the cell lumen presumably reduced.

*ROI 7* The swelling strains of parenchyma cells in ROI 7 are shown in Fig. 5d. The strain of the cell wall increased as RH increased, and that of the cell lumen increased in the parallel direction and decreased in the perpendicular direction. Although the cell in ROI 7 was surrounded by a larger number of parenchyma cells, it was also affected by fibers if they were close enough. Fiber bundles are embedded everywhere in the bamboo culm, and most parenchyma cells might be influenced by them. One parenchyma cell may even be affected simultaneously by several fiber bundles from different vascular bundles, which could result in more complicated changes to the cell lumen.

## Discussions

### Interaction between different cells

The swelling strains of vessel and parenchyma cells show that the deformation and movement of cell lumen were governed by fiber cells. For vessel cell

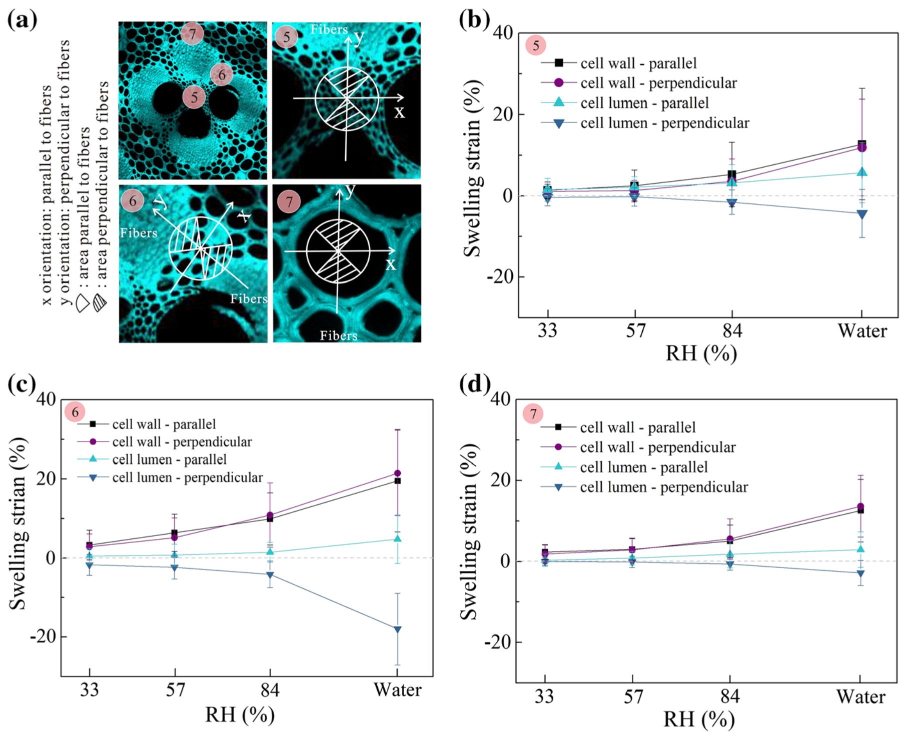


**Fig. 5** **a** Orientations of parenchyma cells in ROIs 5, 6, and 7: x orientation is parallel to fibers while y orientation is perpendicular to fibers; the blank area was defined as the parallel area while the shaded area was defined as the perpendicular area, **b–d** swelling strains of parenchyma cell wall and lumen at ROIs 5, 6, and 7 at different RH conditions

(Item #4 in Fig. 6), at 90° orientations (Fig. 4b), fiber cells were at both ends of the lumen. Fiber cells swell during water adsorption and expand outwards more than inwards due to their small lumen-to-diameter ratio (Table 3). Therefore, the vessel cell was squeezed by fibers from its two ends at 90°, and thus, the lumen shrank. On the contrary, at 0° (or 180°), parenchyma cells were at one end of the lumen. Parenchyma cells have a larger lumen-to-diameter ratio (Table 3) and can bear the deformation arising from the vessel cell. Thus, although vessel cell was squeezed on the fiber cell side, it swelled on the parenchyma cell side and its lumen moved to the right (Item #4 in Fig. 6).

The parenchyma cells were squeezed by the upper fiber bundle if they were in ROI 5 or ROI 7, or

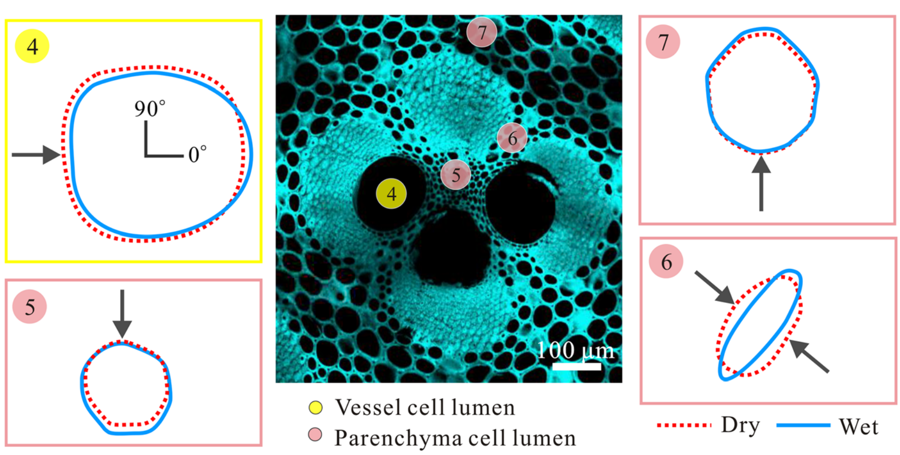


**Fig. 6** Deformation and movement of the lumens of vessel (Item #4 circle) and parenchyma cells (Items #5, 6 and 7) from dry (dot line) to wet (solid line) states in cross-section. The cell lumens always moved to the opposite direction of the fiber bundle

**Table 3** Typical thickness of cell wall, diameter of cell lumen, and lumen-to-diameter ratio of three bamboo cell types (at RH 11%)

| Cell name | CLSM in cross-section | Thickness of the cell wall (μm) | $D_{lumen}$ (μm) | $D_{cell}$ (μm) | Lumen-to-diameter ratio (%) |
|---|---|---|---|---|---|
| Fiber cell | 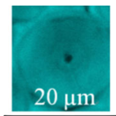  | 8.8 | 1.5 | 19.1 | 7.9 |
| Parenchyma cel[a] | 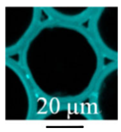  | 4.1 | 38.0 | 46.2 | 82.3 |
| Vessel cell | 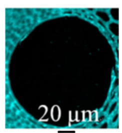  | 1.9 | 121.7 | 125.5 | 97.0 |

[a]The parenchyma cell that is located in the matrix

simultaneously squeezed by the upper and right fiber bundles if they were in ROI 6 (Items #5, 6 and 7 in Fig. 6). The parenchyma cells in ROI 6 were squeezed by the fibers in two directions at the same time, thus the squeeze was approximately twice as large as the cell lumen in ROI 5 or 7, and the resulting shrinkage was also twice as large (Fig. 5).

Fiber bundles acted as an anchor during the process of swelling due to their overwhelming size and mass density (Fig. 6 and Table 3). The lumens of other cells were forced to deform and move to the opposite direction of the fiber bundle. The geometric changes of lumens varied depending on their positions relative to the fiber bundles.

## Comparing the swelling of different cell types

The swelling strain of cell wall was approximately independent of its location or orientation (Figs. 3, 4 and 5), but dependent on the cell type. To compare the swelling of different types of bamboo cells, their absolute and relative swelling per percentage of MC were calculated and the results are shown in Fig. 7a. The absolute swelling per percentage of MC of the cell wall decreased in the following order: fiber > parenchyma > vessel cell. The absolute swelling was directly proportional to the thickness of the cell wall, i.e., the thicker the cell wall, the higher the absolute swelling. The typical thicknesses of fiber, parenchyma, and vessel cells were 8.8 μm, 4.1 μm and 1.9 μm, respectively (Table 3). Therefore, the absolute swelling of fiber cell was higher than that of the other two cells, thus resulting in a higher absolute swelling. The change in cell lumen of the vessel cell was significantly larger than that in the parenchyma cell because of its larger diameter (Table 3).

The relative swelling per percentage of MC is also shown in Fig. 7a. Unlike the absolute swelling, the relative swelling of fiber (0.53%/%) was lower than that of parenchyma (1.1%/%) and vessel cells (1.1%/%). The lumen-to-diameter ratio of fiber cell was 7.9% (Table 3), and the cell wall had little choice but to swell outward after water adsorption. Since a single fiber cell was embedded in the fiber bundle (Fig. 7b), adjacent fiber cells competed against each other for more swelling space. Thus, a part of the swelling stresses was counteracted, and swelling of individual fibers was largely constrained by adjacent fibers. On the contrary, the parenchyma and vessel cells had large lumens for the cell wall to swell inward (Fig. 7c), and thus most of their swelling stresses produced strain. Therefore, the swelling stresses that produced strain were larger in parenchyma and vessel cells than in fiber cell, and the relative swelling was also higher for parenchyma and vessel cells.

At the cell scale, the relative swelling varied widely from − 0.33 to 1.1%/%, due to micro-structural reasons discussed previously in this paper. Zhu et al.

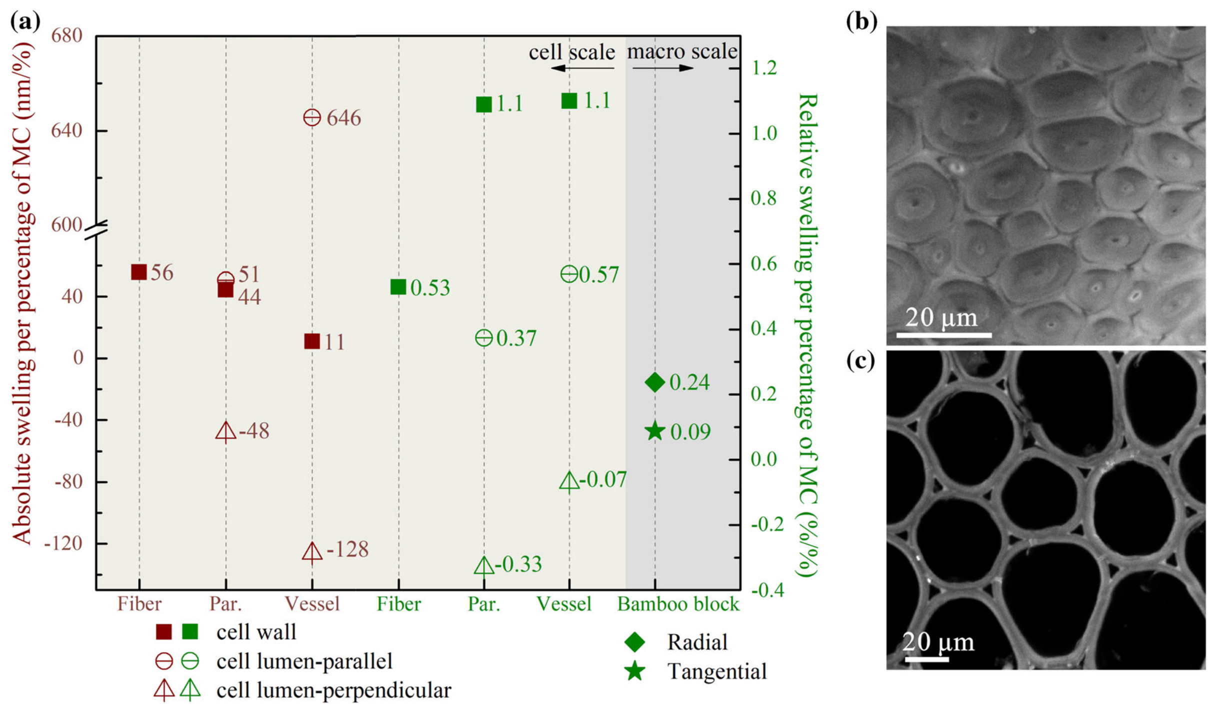


**Fig. 7** **a** Absolute swelling (left) and relative swelling (right) per percentage of MC of different types of cell, and relative swelling per percentage of MC of bamboo block (Zhu et al. 2019; Zhang et al. 2018); **b** and **c** are morphologies of fiber cells and parenchyma cells, respectively

(2019) reported that the swelling of moso bamboo block from oven dry to moisture saturation was approximately 5.3% and 2.0% at the radial and tangential directions, respectively. The fiber saturation point of moso bamboo block was 21.7% (Zhang et al. 2018). Accordingly, the relative swelling per percentage of MC of bamboo block ranged from 0.09 to 0.24%/% (Fig. 7a). These macro-swelling values were somewhat lower than but nevertheless in line with those found in this study at the cellular scale.

## Swelling behavior in T and R directions

At the macro scale, there was no clear difference in swelling/shrinkage in the T and R directions in bamboo (Zhu et al. 2019; Wahab et al. 2012a; Erakhrumen and Ogunsanwo 2009; Anokye et al. 2014), whereas in wood, dimensional change of T direction was undoubtedly larger (Patera et al. 2013; Rafsanjani et al. 2012). Wood cells are rectangular, while bamboo cells are circular in shape (Fig. 8a). Gu et al. (2001) explained the different values of shrinkage between the T and R directions by microfibril angle (MFA). The MFAs of wood cell in the R and T directions were 68.4° and 46.1°, respectively, and the R/T wall thickness ratio was 1.24. Thus, the ratio of differential shrinkage T/R was:

$$\frac{\mathrm{T}}{\mathrm{R}} = \frac{1.24 \times \sin 68.4 + \cos 46.1}{1.24 \times \cos 68.4 + \sin 46.1} = 1.57$$

which was significantly larger than 1. This was one of the main reasons why the wood had a higher T change than R at the macro scale. For moso bamboo (2 years, middle part), the MFAs in the R and T directions were 10.2° and 9.7°, respectively (An 2016). As mentioned previously, the thickness of the bamboo cell wall was similar for different orientations, and thus the R/T wall thickness ratio was approximately 1. The ratio of differential shrinkage T/R was:

$$\frac{\mathrm{T}}{\mathrm{R}} = \frac{1 \times \sin 10.2 + \cos 9.7}{1 \times \cos 10.2 + \sin 9.7} = 1.01$$

which was close to 1. This indicates that compared with wood, the difference between T and R swelling/shrinkage was insignificant for the individual bamboo cell.

**Fig. 8** **a** Micro fibril angles of wood cell and bamboo cell at cellular level; **b** angles of different vascular bundles were random on the cross-section at tissue level

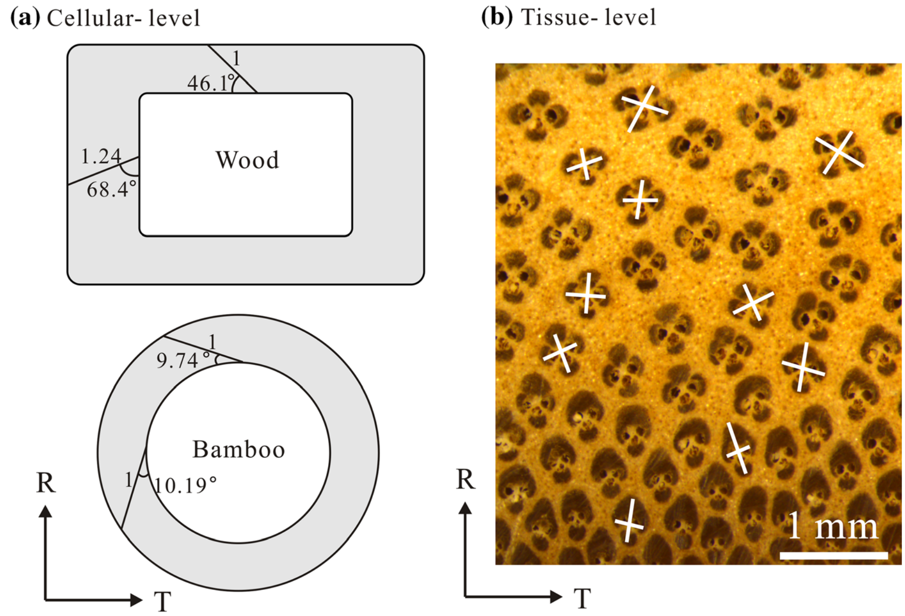


As demonstrated earlier, the swelling of bamboo cells was mainly controlled by the fiber bundles. At the tissue level, fiber bundles are embedded randomly in the parenchyma ground tissue along the radial direction of bamboo culm. In addition, as shown in Fig. 8b, the embedded angles of different vascular bundles were also random. This implies that the angular effect of fiber bundles is random, which results in arbitrary swelling in the T and R directions at the macro scale.

## Conclusions

The swelling behaviors of moso bamboo cells (fiber, parenchyma and vessel cells) were investigated. The results show that the swelling strain of cell wall increased with the increase of RH, and was independent of its location and orientation, but dependent on the cell type. The absolute swelling of cell wall was positively influenced by the cell wall thickness and was about 56 nm for every percentage of MC increase for fiber cells, 44 nm for parenchyma cells and 11 nm for vessel cells. On the other hand, due to constraint of its adjacent fibers, the relative swelling of fiber cell wall was 0.53% for every percentage of MC increase. This value was almost of half of 1.1% relative swelling for parenchyma and vessel cells. The deformation and movement of cell lumens of parenchyma and vessel cells were influenced by their geometric positions in relation to fiber bundles. The cell lumen increased with RH when it was parallel to the fibers, and decreased when it was perpendicular to the fibers. In contrast to wood, there was a lack of differential swelling in bamboo in the tangential and radial directions, due to the similar microfibril angle in both directions, the circular cellular shape and the random embedment of vascular bundles. While the numerical results found in this study may vary depending on species and age of bamboo, the general swelling mechanisms and relationships should be applicable to all bamboo fibers.

**Acknowledgments** The authors gratefully acknowledge financial support from 13th Five-Year the National key Research and Development projects (2016YFD0600906) and the Fundamental Research Funds for the International Centre for Bamboo and Rattan (1632017001). This study is supported by Zhejiang Xinzhou Bamboo-based Composites Technology Co., Ltd. and support of FPInnovations is also gratefully acknowledged.

## References

Ahmad M, Kamke FA (2005) Analysis of Calcutta bamboo for structural composite materials: physical and mechanical properties. Wood Sci Technol 39(6):448–459

An X (2016) Microfibril orientations and ultrastructures of fibers wall from Moso bamboo. Dissertation, Chinese Academy of Forestry

Anokye R, Kalong RM, Bakar ES, Ratnasingam J, Jawaid M, Awang K (2014) Variations in moisture content affect the shrinkage of Gigantochloa scortechinii and Bambusa vulgaris at different heights of the bamboo culm. BioResources 9(4):7484–7493

Chen G, Luo H, Yang H, Zhang T, Li S (2018) Water effects on the deformation and fracture behaviors of the multi-scaled cellular fibrous bamboo. Acta Biomater 65:203–215

Chen Q, Dai C, Fang C, Chen M, Zhang S, Liu R, Liu X, Fei B (2019) Mode I interlaminar fracture toughness behavior and mechanisms of bamboo. Mater Des 183:108132

Du K, Li S, Zhao L, Qiao L, Ai H, Liu X (2018) One-step growth of porous cellulose beads directly on bamboo fibers via oxidation-derived method in aqueous phase and their potential for heavy metal ions adsorption. ACS Sustain Chem Eng 6(12):17068–17075

Erakhrumen AA, Ogunsanwo OY (2009) Water absorption, anti-swell efficacy, and dimensional stability properties of neem seed oil-treated wild grown Bambusa vulgaris Schrad. ex JC Wendl. in Southwest Nigeria. BioResources 4(4):1417–1429

Fang C, Jiang Z, Sun Z, Liu H, Zhang X, Zhang R, Fei B (2018) An overview on bamboo culm flattening. Constr Build Mater 171:65–74

Gu H, Zink-Sharp A, Sell J (2001) Hypothesis on the role of cell wall structure in differential transverse shrinkage of wood. Eur J Wood Wood Prod 59(6):436–442

Habibi MK, Samaei AT, Gheshlaghi B, Lu J, Lu Y (2015) Asymmetric flexural behavior from bamboo's functionally graded hierarchical structure: underlying mechanisms. Acta Biomater 16:178–186

Jiang Z (2007) Bamboo and rattan in the world. China Forestry Pub House, Beijing

Khalil HA, Mohamad HC, Khairunnisa AR, Owolabi FAT, Asniza M, Samsul R, Nurul FM, Paridah MT (2018) Development and characterization of bamboo fiber reinforced biopolymer films. Mater Res Express 5(8):085309

Le Phuong HA, Ayob NAI, Blanford CF, Mohammad Rawi NF, Szekely G (2019) Non-woven membrane supports from renewable resources: bamboo fiber reinforced poly (Lactic Acid) composites. ACS Sustain Chem Eng 7:11885–11893

Lv H, Ma X, Zhang B, Chen X, Liu X, Fang C, Fei B (2019) Microwave-vacuum drying of round bamboo: a study of the physical properties. Constr Build Mater 211:44–51

Patera A, Derome D, Griffa M, Carmeliet J (2013) Hysteresis in swelling and in sorption of wood tissue. J Struct Biol 182(3):226–234

Rafsanjani A, Derome D, Wittel FK, Carmeliet J (2012) Computational up-scaling of anisotropic swelling and mechanical behavior of hierarchical cellular materials. Compos Sci Technol 72(6):744–751

Rafsanjani A, Lanvermann C, Niemz P, Carmeliet J, Derome D (2013) Multiscale analysis of free swelling of Norway spruce. Compos Part A Appl Sci Manuf 54:70–78

Rafsanjani A, Stiefel M, Jefimovs K, Mokso R, Derome D, Carmeliet J (2014) Hygroscopic swelling and shrinkage of latewood cell wall micropillars reveal ultrastructural anisotropy. J R Soc Interface 11(95):1–10

Ribeiro RAS, Ribeiro MGS, Sankar K, Kriven WM (2016) Geopolymer-bamboo composite–A novel sustainable construction material. Constr Build Mater 123:501–507

Sakagami H, Matsumura J, Oda K (2007) Shrinkage of tracheid cells with desorption visualized by confocal laser scanning microscopy. IAWA 28(1):29–37

Taguchi A, Murata K, Nakano T (2010) Observation of cell shapes in wood cross-sections during water adsorption by confocal laser-scanning microscopy (CLSM). Holzforschung 64(5):627–631

Taguchi A, Murata K, Nakamura M, Nakano T (2011) Scale effect in the anisotropic deformation change of tracheid cells during water adsorption. Holzforschung 65(2):253–256

Wahab R, Mustafa MT, Rahman S, Salam MA, Sulaiman O, Sudin M, Rasat M (2012a) Relationship between physical, anatomical and strength properties of 3-year-old cultivated tropical bamboo Gigantochloa scortechinii. ARPN J Agric Biol Sci 7(10):782–791

Wahab R, Mustafa MT, Salam MA, Tabert TA, Sulaiman O, Sudin M (2012b) Potential and structural variation of some selected cultivated bamboo species in Peninsular Malaysia. International Journal of Biology 4(3):102–116

Wegst UG (2008) Bamboo and wood in musical instruments. Annu Rev Mater Res 38:323–349

Yamashita K, Hirakawa Y, Nakatani H, Ikeda M (2009) Tangential and radial shrinkage variation within trees in sugi (*Cryptomeria japonica*) cultivars. J Wood Sci 55(3):161–168

Yang S, Jiang Z, Ren H, Fei B, Liu X (2011) Comparative Anatomy Study of 6 Bamboo Species. Trans China Pulp Pap 26(2):11–15

Zhang X, Li J, Yu Y, Wang H (2018) Investigating the water vapor sorption behavior of bamboo with two sorption models. J Mater Sci 53(11):8241–8249

Zhu J, Wang H, Wang C (2019) Study on the swelling characteristics of bamboo based on its graded hierarchical structure. Wood Fiber Sci 51(3):332–342

**Publisher's Note** Springer Nature remains neutral with regard to jurisdictional claims in published maps and institutional affiliations.